Journal of Thermal Analysis and Calorimetry, Vol. 88 (2007) 1, 177–180

DSC CHARACTERISATION OF CHEMICALLY REDUCED ELECTROLYTIC MANGANESE DIOXIDE

B. Liu[1], *P. S. Thomas*[1*], *A. S. Ray*[1], *R. P. Williams*[2] *and S. W. Donne*[3]

[1]Department of Chemistry, Materials and Forensic Sciences, University of Technology Sydney, PO Box 123 Broadway, NSW 2007, Australia
[2]Delta-EMD Australia Pty Limited, McIntosh Drive, Mayfield West, 2304, Australia
[3]Discipline of Chemistry, University of Newcastle, Callaghan, NSW 2308, Australia

The thermal decomposition of electrolytic manganese dioxide (EMD), in an inert atmosphere, and the effect of chemical reduction on EMD, using 2-propanol under reflux (82°C), was investigated by differential scanning calorimetry (DSC). This study is an extension of a study investigating the thermal decomposition of EMD and reduced EMD by TG-MS (J. Therm. Anal. Cal., 80 (2005)625)). The DSC characterisation was carried out up to 600°C encompassing the water loss region up to 390°C and the first thermal reduction step. Water removal was observed in two distinct endothermic peaks (which were not deconvolved in the TG-MS) associated with the removal of bound water. For the lower degrees of chemical reduction, thermal reduction resulted in the formation of Mn_2O_3; for higher degrees of chemical reduction, the thermal reduction resulted in Mn_3O_4 at 600°C. In the DSC the thermal reduction of the EMD and chemically reduced specimen was observed to be endothermic. The reduced specimens, however, also showed an exothermic structural reorganisation.

Keywords: *chemical reduction, DSC, electrolytic manganese dioxide*

Introduction

Electrolytic manganese dioxide (EMD), the dominant cathode material used in dry cell alkaline batteries, is produced by anodic electrolytic deposition from solution [1]. EMD has the γ-MnO_2 crystal structure which is a blend or intergrowth of pyrolusite (β-MnO_2) and ramsdellite domains. The performance of EMD as a cathode material is dependent on a variety of factors including the morphology, crystallinity and porosity as well as the water content and character of the water in the specimen [1, 2]. These factors are of importance in determining the performance of EMD in application as the mechanism of charge transfer is based on the intercalation of protons into the γ-MnO_2 structure as the EMD is reduced:

$$MnOOH_r+\Delta H_2O+\Delta e^- \longrightarrow MnOOH_{r+\Delta}+\Delta OH^- \quad (1)$$

where '*r*' in Eq. (1) represents the level of proton insertion [1, 2]. The reduction and intercalation of protons into the structure is topotactic in nature up to a value of r=0.7 [1]. Above this value, δ-MnOOH is formed as a separate phase, with similar structural characteristics to that of the EMD, but in this case, with an intergrowth of the α- and γ-MnOOH phases [3]. The electrochemical performance (i.e. the ease of progression of Eq. (1)), or the rechargeablility (i.e. reversibility of Eq. (1)), is strongly dependent on phase behaviour as well as the morphological factors described above [1].

The phase behaviour and morphological character of EMD can be characterised by thermal methods as thermal methods are sensitive to morphological character through their dynamic nature and are sensitive to phase morphology through the thermal activation of thermodynamic processes. Thermal methods applied to the characterisation of EMD have yielded both the character of the water contained in EMD and the steps involved in the thermal reduction of EMD in accordance with the general scheme given by Eq. (2) [4–7].

$$MnO_2\cdot nH_2O \xrightarrow{0} MnO_2 \xrightarrow{I} Mn_2O_3 \xrightarrow{II} \xrightarrow{II} Mn_3O_4 \xrightarrow{III} MnO \quad (2)$$

Step *O* (identified here as *O* for consistency with the literature) corresponds to the loss of water. It should be noted that partially reduced manganese dioxides will result in the presence of Mn(III) ions in the lattice. Step *O* may, therefore, be more accurately described by Eq. (6) below. Three classes of water have been identified using thermogravimetric (TG) analysis: physisorbed water (Type I), reversibly removed around 100°C, surface bound hydroxyls and water of crystallisation (Type II), irreversibly removed around 200°C, and bulk hydroxyl groups (Type III), removed, irreversibly, around 300°C [4, 7]. Above

* Author for correspondence: paul.thomas@uts.edu.au

1388–6150/$20.00

Akadémiai Kiadó, Budapest, Hungary
Springer, Dordrecht, The Netherlands

400°C, the thermal reduction of EMD takes place [5–7] with Step I occurring in the range 460 to 570°C, Step II in the range 700 to 800°C and Step III above 1300°C. The actual mechanism for the thermal reduction, and the temperature at which it occurs, of manganese oxides is known to be a function of the origin and history of the specimen as well as the environment in which the reduction is carried out [5, 6, 8]. For the thermal decomposition of EMD some of these steps, in particular Step I, have been shown to be a complex series of reduction processes through intermediate stoichiometric compositions [6, 7, 9, 10]. It is this region, below 600°C, which is the subject of this paper and is investigated through the thermal decomposition of both as received EMD and chemically reduced EMD using differential scanning calorimetry (DSC).

Experimental

EMD was supplied by Delta EMD Australia Pty Limited and was determined to be γ-MnO_2 by X-ray diffraction (XRD) analysis. Samples of the EMD were chemically reduced under reflux (82°C) in AR grade 2-propanol for 1, 2, 3, 6, and 24 h [7]. The reduced EMD specimens were recovered by filtration and thoroughly washed with acetone, vacuum dried and stored in a desiccator. The determination of *r* in Eq. (1), i.e. the degree of reduction, was carried out based on the potentiometric titration method described by Vetter and Jaeger [11] and are listed in Table 1. XRD data of the specimens reduced from 1 to 3 h showed only isotropic expansion of the γ-MnO_2 lattice. The 6 h specimen showed signs of δ-MnOOH in the XRD data with significant proportions of δ-MnOOH observed in the 24 h reduced specimen [7].

DSC characterisation was carried out using a TA Instruments 2920 MDSC. Samples (20.0±0.1 mg) were placed in an aluminium pan without crimping a lid onto the pan so that the pan was left 'open' to the atmosphere of the DSC cell. The samples were then heated at a rate of 5°C min^{-1} from ambient temperature to 600°C under flowing (150 mL min^{-1}) high purity nitrogen (BOC, <10 ppm oxygen).

Results and discussion

The DSC data for the thermal reduction of EMD and specimens of EMD which were chemically reduced are shown in Fig. 1. The peak positions are shown in Table 1. This corresponds well with the DTG data reported previously [7] and are included here for comparison in Fig. 2. The data in Figs 1 and 2 correspond to temperature range of Steps *O* and *I* of

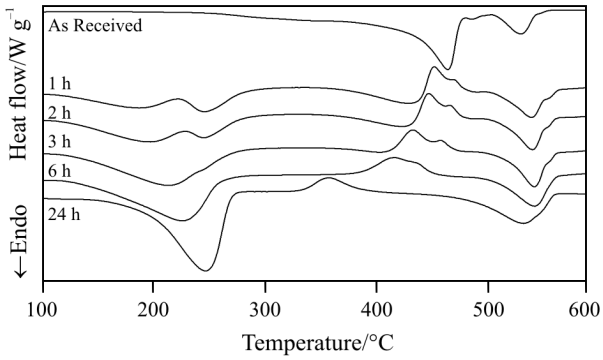

Fig. 1 DSC curves for EMD and specimens of EMD chemically reduced by reflux in isopropanol

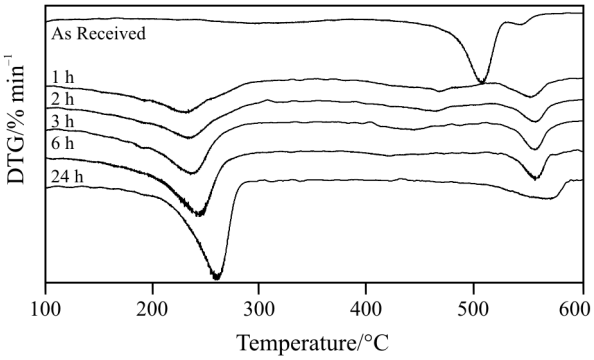

Fig. 2 DTG curves reported in [7] for the samples included in Fig. 1

Eq. (2). For the as received EMD the onset of an endotherm is observed at approximately 240°C and corresponds to the removal of bound water from the EMD (Step *O*) [7]. The removal of water is observed to overlap with the onset of the thermal reduction process, Step I, as confirmed by the observation of oxygen in the evolved gas analysis (EGA) reported in [7]. Step I is observed to be quite complex, for the as received EMD, with two major peaks observed in the decomposition with at least two minor peaks also evident. This decomposition step has been reported to occur through an intermediate based on the identification of phases by XRD [6]:

$$7MnO_2 \longrightarrow Mn_5O_8 + Mn_2O_3 + 3/2O_2 \quad (3)$$

$$2Mn_5O_8 \longrightarrow 5Mn_2O_3 + 1/2O_2 \quad (4)$$

The thermal decomposition of the reduced specimens in this region is observed to be significantly different to that of the as received EMD. The DTG data shows a single peak in the water removal region with increasing size of the peak corresponding to increasing degree of reduction. The DSC shows, for low degree of reduction (1 and 2 h reflux reduction samples), two peaks in this region which are likely to correspond to the Lee *et al.* [4] water Types II and III, although the peak temperatures are lower. The two

Table 1 Peak positions in the DSC curves in Fig. 1 The peak positions of the DTG curves in Fig. 2 are given in brackets below the DSC data

Sample	r in $MnOOH_r$	Water loss endotherm/°C		Exotherm/°C		$MnO_2 \rightarrow Mn_2O_3$/°C	
		Peak 1	Peak 2 (DTG)	Peak 1	Peak 2	Peak 1 (DTG)	Peak 2 (DTG)
Unreduced	0.10	–	–	–	–	474	541
			(310)			(507)	(544)
1 h	0.48	191	251	461	479	–	550
			(232)			(468)	(554)
2 h	0.60	200	250	456	475	–	551
			(237)			(462)	(557)
3 h	0.64	218	248	441	467	–	553
			(238)			(442)	(557)
6 h	0.68	231	–	425	442	–	553
			(244)			(421)	(558)
24 h	0.92	–	251	364		–	543
			(262)				(566)

types of bound water observed merge into a single peak as the degree of reduction increases. Only a single peak in this region is observed in the DTG and can be ascribed to configurational differences between the experiment types [6]. Differences in the peak positions between the DSC and DTG data can be similarly explained.

Although in the region below 390°C only water loss from the 24 h reduced sample was reported in the EGA data, XRD data indicated that the decomposition resulted in a mixture of Mn_3O_4 and Mn_5O_8 at 310°C [7]. The decomposition products are, therefore, consistent with disproportionation of the MnOOH present [7, 9, 10].

$$8MnOOH \longrightarrow Mn_3O_4 + Mn_5O_8 + 4H_2O \qquad (5)$$

The DSC (and DTG) curves for Step I of Eq. (2) for the reduced specimens were observed to be significantly different to that of the as received EMD. The decomposition product observed at 600°C, however, was Mn_2O_3 for each of the chemically reduced specimens (with the exception of the 24 h reduced specimen which formed Mn_3O_4). Evidence of Mn_5O_8 was also observed as an intermediate suggesting that some form of Eqs (3) and (4) are adhered to [7]. Agopsowicz *et al.* [10] proposed:

$$(1\text{-}r)MnO_2 \cdot r MnOOH \longrightarrow$$
$$\longrightarrow \frac{r}{4}Mn_5O_8 + \frac{r}{2}H_2O + \left(\frac{4-5r}{4}\right)MnO_2 \qquad (6)$$

to account for reduction in the topotactic regime of proton insertion, where r represents the degree of reduction as defined by Eq. (1). Equation 6 suggests that the limit of insertion of protons in the γ-MnO_2 lattice occurs at a value of r=0.8. The limit is probably dependent on the specific γ-MnO_2 specimen as the presence of δ-MnOOH for the specimens used in this study was reported for value of r=0.68 [7]. The MnO_2 subsequently decomposes via the stoichiometry given by Eq. (3) and the Mn_5O_8 via that given by Eq. (4).

For the 24 h specimen, Mn_2O_3 was not identified as a product of thermal decomposition and only a single peak at 560°C was observed in the DSC or DTG data. XRD analysis indicated the presence of both Mn_5O_8 and Mn_3O_4 at 430°C, but, at 600°C, only Mn_3O_4 was observed corresponding to the decomposition of Mn_5O_8 to Mn_3O_4 as has been reported elsewhere for the thermal decomposition of δ-MnOOH [10]:

$$3Mn_5O_8 \rightarrow 5Mn_3O_4 + 2O_2 \qquad (7)$$

The DSC data also has a prominent exothermic transformation which is observed for each of the reduced specimens; around 470°C for the 1 h reduced specimen, decreasing to approximately 360°C for the 24 h reduced specimen. Although exothermic transformations have been reported in the literature for the reduction of hydrated MnO_2 under reactive atmospheres [4, 12], and inert atmospheres for manganese dioxides containing >10 mol% of potassium ions [13], exothermic transformations have not been reported for EMD or reduced EMDs. The as received EMD showed, as expected, no exothermic transformation in the heat flow curve. The reduced specimens all show a prominent exotherm. For the 1, 2 and 3 h specimens, the exotherm is superimposed on an endotherm. In each case there is a small mass loss associated with a small broad DTG peak which is observed before the main decomposition

process for Step I. In the 6 hour reduced specimen evidence of a very small DTG peak is observed, but no endotherm is apparent coinciding with the exotherm. For the 24 h case, no mass loss is observed in the region of the exotherm. The exotherm is, therefore, likely to be associated with a structural reorganisation rather than a decomposition process. γ-MnO_2 has been observed to transform to β-MnO_2 prior to the decomposition Step I [5, 6]. As the chemically reduced specimens of EMD retain their stacking faults to form the EMD equivalent of δ-MnOOH [3, 9], it is likely that a similar structural reorganisation is taking place prior to the decomposition step.

Conclusions

The thermal characterisation of EMD and chemically reduced EMD by DSC up to 600°C has allowed the further characterisation of two decomposition steps of Eq. (2); the removal of bound water, Step O, and the thermally induced reduction to lower oxidation state manganese oxides, Step I. The reduced specimens clearly showed the presence of two types of water which were ascribed to be due to the removal of bound water (Types II and III [4, 7]). The thermal reduction occurring during Step I produced the expected endotherms associated with reduction of the MnO_2 (and $MnOOH_r$) to lower oxidation state oxides. Unexpectedly, an exotherm was observed during the thermal reduction of the chemically reduced specimens which was ascribed to structural rearrangement rather than decomposition as the peak was observed to overlap with an endotherm when mass loss was observed; when no mass loss was observed only the exotherm was present. The transformation has not been assigned but is likely to be similar to the reported γ- to β-MnO_2 transformation [5, 6].

References

1 S. Donne, R. Fredlein, G. Lawrance, D. Swinkels and F. L. Tye, Prog. Batteries Battery Mater., 13 (1994) 113.
2 J. Fitzpatrick and F. L. Tye, J. Appl. Electrochem., 21 (1991) 130.
3 W. C. Maskel, J. E. A. Shaw and F. L. Tye, Electrochim. Acta, 26 (1981) 1403.
4 J. A. Lee, C. E. Newnham and F. L. Tye, J. Colloid Interface Sci., 42 (1973) 372.
5 B. D. Desai, J. B. Fernandes and V. N. K. Dalal, J. Power Sources, 16 (1985) 1.
6 B. Liu, P. S. Thomas, A. S. Ray and R. P. Williams, J. Therm. Anal. Cal., 76 (2004) 115.
7 B. Liu, P. S. Thomas, A. S. Ray and R. P. Williams, J. Therm. Anal. Cal., 80 (2005) 625.
8 R. Giovanoli, Prog. Batteries Battery Mater., 13 (1994) 50.
9 J. A. Lee, C. E. Newnham, F. S. Stone and F. L. Tye, J. Solid State Chem., 31 (1980) 81.
10 A. Agopsowicz, J. L. Hitchcock and F. L. Tye, Thermochim. Acta, 32 (1979) 63.
11 N. Jaeger and K. J. Vetter, Electrochim. Acta, 11 (1966) 401.
12 Gonzalez, J. I. Gutierrez, J. R. Gonzalez-Velasco, A. Cid, A. Arranz and J. F. Arranz, J. Thermal Anal., 52 (1998) 985.
13 E. Narita and T. Okabe, Bull. Chem. Soc. Jpn., 53 (1980) 525.

DOI: 10.1007/s10973-006-8132-y